Circuitry Design and Magnetic Susceptibility Evaluation of 7T fMRI Implantable RF Coil

Rong Wang, Celia M. Dong, Ed X. Wu, Robert C. Roberts, and Li Jun Jiang

Department of Electrical and Electronic Engineering
The University of Hong Kong, City, Pokfulam Road, Hong Kong
wang1130@hku.hk

Abstract ─ Implantable coils have been widely utilized in functional magnetic resonance imaging (fMRI) owing to their superior signal to noise ratio. To effectively minimize the magnetic field distortion and image artifacts, the magnetic susceptibility of the implantable coil needs to be evaluated before practical use. In this work, we experimentally identify the magnetic susceptibility of each component of the implantable coil with the 7T Bruker NMR imaging scanner and provide useful guidelines for the following manufacturing. A 5×5 mm^2 implantable surface coil with a tunable frequency range is subsequently introduced for the 7T fMRI of the rat primary somatosensory cortex (S1FL). A detachable external tuning circuit for the implantable coil is employed to facilitate in-vivo measurements in the rat model.

Index Terms ─ fMRI, implantable coil, magnetic susceptibility.

I. INTRODUCTION

Radio frequency coils have become indispensable components for the magnetic resonance imaging (MRI) scanners owing to their ability to transmit RF pulse at the Larmor frequency and receive the free induction decay signal [1], [2]. The recent discovery that MRI could be utilized for sensing neural activity (also known as Functional MRI or fMRI) has greatly spurred the research and development of the miniaturized and implantable coils [3], [4]. In contrast with conventional T2-weighted MRI, fMRI sets stringent requirement of the magnetic susceptibility for the implantable coil since the fast image acquisition technique adopted such as echo planar imaging (EPI) is less tolerant of the magnetic field distortion induced by the implantable coil and tends to bring in susceptibility artifacts which diminish the quality of the retrieved image. Therefore, the magnetic susceptibility evaluation of each component of the implantable coil is crucial before system assembly and measurement. In this paper, a 5×5 mm^2 implantable planar coil is designed and manufactured for 7T fMRI of the rat S1FL cortex region. As shown in the flowchart of Fig. 1 (a), after the circuitry design and simulation process, the magnetic susceptibility of all the components of the implantable coil are evaluated by capturing their EPI images within the cylindrical homogeneous saline phantom. The implantable coil is then carefully assembled following the guidelines offered by the magnetic susceptibility evaluation and finally connected with an external tuning circuit to experimentally function at 300 MHz, the Larmor frequency of 7T scanner.

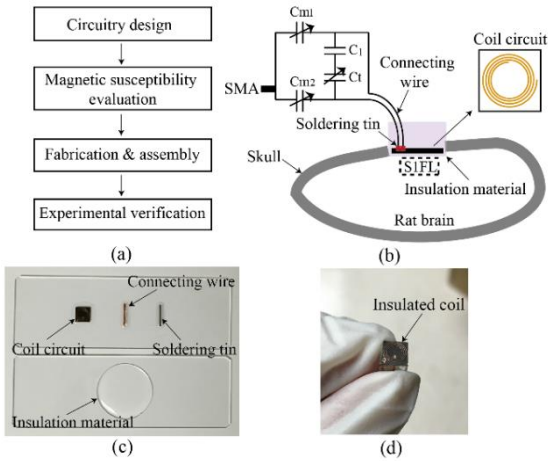

Fig. 1. (a) Flowchart of coil design, (b) schematic diagram of the proposed implantable coil, (c) samples of the coil components on glass slides, and (d) snapshot of the assembled coil.

II. CIRCUITRY DESIGN

The circuitry is mainly composed of an implantable coil and a tuning circuit. The proposed surface coil is constituted by four components, coil circuit, copper connecting wire, insulation material and soldering tin as shown in Fig. 1 (b). The substrate of the coil circuit is 0.254 mm thick Rogers 5880 laminate. The insulation material is Polydimethylsiloxane (PDMS) which is exhaustively used in implantable devices for electrical

Submitted On: September 22, 2018
Accepted On: October 12, 2018

sealing.

The simulated inductance and intrinsic resistance of the proposed 5 × 5 mm^2 four-turn planar coil (35 um thick copper trace, 0.127 mm trace width and spacing) are 67.2 nH and 0.38 Ω respectively, obtained from ANSYS Maxwell. Note that the Larmor frequency should be indicated in the simulation to obtain the additional resistance caused by the skin effect. The surface coil is then represented by an equivalent circuit in Agilent ADS simulator and the ranges of the variable matching and tuning capacitors C_m and C_t are further determined. In this design, the tuning circuit is constituted by a fixed capacitor C_1=2 pF and three identical trimmer capacitors C_{m1}, C_{m2} and C_t (tuning range: 1.8 to 4.5 pF, non-magnetic surface mount SGC3 series, manufactured by Sprague-Goodman).

III. MAGNETIC SUSCEPTIBILITY EVALUATION

Magnetic susceptibility χ_m is a measure indicating the magnetization extent of a material under external magnetic field. The magnetic induction **B** is related to χ_m by the relationship:

$$\mathbf{B} = \mu_0(1 + \chi_m)\mathbf{H},$$

where μ_0 is vacuum permeability and **H** is the magnetic field strength. For implantable coil, the extra magnetic induction **B** induced by its magnetic susceptibility χ_m will distort the base magnetic induction $\mathbf{B}_0$ and vary the base Larmor frequency f_0 which is proportional to $\mathbf{B}_0$. The frequency deviation, in turn, produces signal loss and brings in susceptibility artifacts to the retrieved image. Compared with the time-consuming T2-weighted MRI process, fMRI sacrifices the magnetic susceptibility tolerance to reduce the image acquisition time and capture the instant change of the neural activity.

Therefore, for fMRI application, the evaluation of the magnetic susceptibility of the elements and materials that constitute the implantable coil should be conducted before the manufacture and assembly process. In this work, we take a piece of every coil construction component and place it on glass slide as shown in Fig. 1 (c). Both T2 and EPI images of every piece immersed in a cylindrical homogeneous saline phantom are captured by the high-field 7T Bruker NMR imaging scanner. The induced susceptibility artifacts of each component could be easily identified by comparing its T2 and EPI images in Fig. 2. The susceptibility artifacts produced by the soldering tin is more significant over the other three, visually indicated by the distorted EPI image of the glass slide underneath soldering tin. Thus, particular attention should be paid to the amount of the soldering tin during fabrication. The image of the assembled implantable coil is shown in Fig. 1 (d). The whole implantable surface coil is totally wrapped with PDMS and electrically insulated from the rat brain.

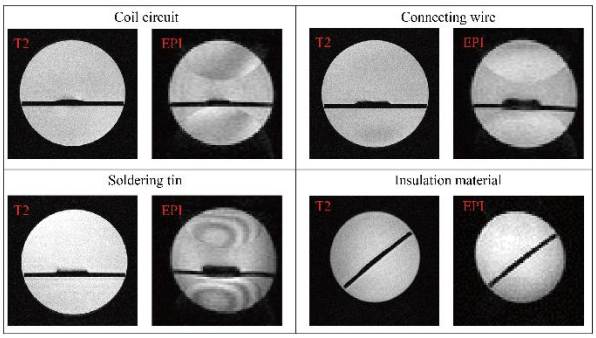

Fig. 2. T2 and EPI images of implantable coil components acquired by the high-field 7T Bruker NMR imaging scanner.

IV. MEASUREMENT

To facilitate the brain surgery for coil implantation, the implantable coil and the external tuning circuit are designed to be detachable with the aid of a plug-in detachable connector as shown in Fig. 3 (a). In Fig. 3 (b), the frequency tuning range is first measured in vacuum and the working frequency could be tuned to 300 MHz with S_{11} = -20.1 dB. A continuous range from 288 to 342 MHz is obtained (S_{11} < -15 dB) by tuning the variable capacitors. Furthermore, this tuning range is examined in an extreme case when the sealed coil is immersed in saline since the permittivity of saline (ε_r=78.4) is much larger than these of brain tissues, such as cerebral cortex and skull [5]. Here, the continuous tuning range shifts to 266 and 306 MHz and still covers the Larmor frequency of 300 MHz, validating the effectiveness of this surface coil for brain implantation.

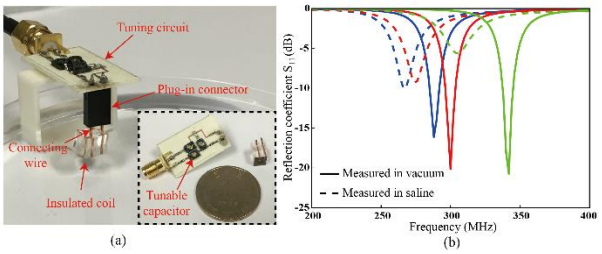

Fig. 3. (a) Photograph of the implantable surface coil immersed in saline. The inset shows the detachable tuning circuit and coil. (b) Measured reflection coefficient and tunable frequency range in vacuum and saline.

V. CONCLUSION

This paper carries out both circuitry design and magnetic susceptibility evaluation of an implantable, tunable and detachable surface coil for the 7T fMRI of the rat cortex region. The experimentally identified magnetic susceptibility of each component provides useful guidelines for the implantable fMRI coil design

and fabrication.

ACKNOWLEDGMENT

This work is supported by the Seed Fund of University Grants Council of Hong Kong (No. AoE/P-04/08) and Hong Kong Research Grants Council grant (C7048-16G).

REFERENCES

[1] C. Massin, G. Boero, F. Vincent, J. Abenhaim, P-A. Besse, and R. S. Popovic, "High-Q factor RF planar microcoils for micro-scale NMR spectroscopy," *Sens. Actuators, A*, vol. 97, pp. 280-288, Apr. 2002.

[2] S. Eroglu, B.Gimi, B. Roman, G. Friedman, and R. L. Magin, "NMR spiral surface microcoils: Design, fabrication, and imaging," *Concepts in Magnetic Resonance Part B: Magnetic Resonance Engineering*, vol. 1, pp. 1-10, Apr. 2003.

[3] L. Renaud, M. Armenean, L. Berry, P. Kleimann, P. Morin, M. Pitaval, J. OBrien, M. Brunet, and H. Saint-Jalmes, "Implantable planar RF microcoils for NMR microspectroscopy," *Sens. Actuators, A*, vol. 99, pp. 244-248, June 2002.

[4] M. Bilgen, I. Elshafiey, and P. A. Narayana, "In vivo magnetic resonance microscopy of rat spinal cord at 7T using implantable RF coils," *Magn. Reson. Med.*, vol. 46, pp. 1250-1253, Nov. 2001.

[5] S. Wood and T. S. Ibrahim, "Design and fabrication of a realistic anthropomorphic heterogeneous head phantom for MR purposes," *PloS One*, vol. 12, pp. 0183168, Aug. 2017.